A&A 532, A148 (2011)
DOI: 10.1051/0004-6361/201116742

Astronomy & Astrophysics

A large Hα line forming region for the massive interacting binaries β Lyrae and υ Sagitarii

D. Bonneau[1], O. Chesneau[1], D. Mourard[1], Ph. Bério[1], J. M. Clausse[1], O. Delaa[1], A. Marcotto[1], K. Perraut[2], A. Roussel[1], A. Spang[1], Ph. Stee[1], I. Tallon-Bosc[3], H. McAlister[4,5], T. ten Brummelaar[5], J. Sturmann[5], L. Sturmann[5], N. Turner[5], C. Farrington[5], and P. J. Goldfinger[5]

[1] Lab. H. Fizeau, Univ. Nice Sophia Antipolis, CNRS UMR 6525, Obs. de la Côte d'Azur, Av. Copernic, 06130 Grasse, France
e-mail: Daniel.Bonneau@oca.eu
[2] UJF-Grenoble 1/CNRS-INSU, Inst. de Planétologie et d'Astrophysique de Grenoble (IPAG) UMR 5274, Grenoble 38041, France
[3] Univ. Lyon 1, Observatoire de Lyon, 9 avenue Charles André, Saint-Genis Laval 69230, France
[4] Georgia State University, PO Box 3969, Atlanta GA 30302-3969, USA
[5] CHARA Array, Mount Wilson Observatory, 91023 Mount Wilson CA, USA

Received 17 February 2011 / Accepted 1 July 2011

ABSTRACT

Aims. This study aims at constraining the properties of two interacting binary systems by measuring their continuum-forming region in the visible and the forming regions of some emission lines, in particular Hα, using optical interferometry.
Methods. We have obtained visible medium ($R \sim 1000$) spectral resolution interferometric observations of β Lyr and of υ Sgr using the VEGA instrument of the CHARA array. For both systems, visible continuum (520/640 nm) visibilities were estimated and differential interferometry data were obtained in the Hα emission line at several epochs of their orbital period. For β Lyr, dispersed visibilities and phases were also obtained in the Hβ and the HeI 6678 Å lines.
Results. As expected, for baselines shorter than 60 m, the system of β Lyr is unresolved in the visible continuum, but the source associated with the Hα, the Hβ and the HeI 6678 Å lines appears to be well resolved at any orbital phase. The differential visibilities through these lines are lower during eclipses, indicating that significant emission originates close to the stars. The Hα line forming region appears to be made up of a compact source located near the orbital plane (possibly linked with the "hot point") and an extended source (i.e. ≥2 mas, i.e. 125 $R_\odot$) out of the orbital plane (possibly associated to the "jet-like feature"). The υ Sgr continuum visibilities are at a similar level for short (20–25 m) and long (90–110 m) baselines. This is interpreted as the presence of an extended structure surrounding a compact bright source. No binary signal was detected, excluding a flux ratio between the stellar components of the system larger than 0.1 from 500 to 700 nm. The radius of the brightest star is estimated to be 0.33 ± 0.16 mas, i.e. 21 ± 10 $R_\odot$ using the latest Hipparcos distance. By contrast, the Hα line forming region is very extended (i.e. ≥6 mas, i.e. 400 $R_\odot$) and found to be off-center from the brightest star, following the orbital motion of the hidden companion.
Conclusions. In both cases, the extension of the Hα line forming region is much larger than the size of the system, which is indicative of a non-conservative evolution. Although a large circumbinary disk surrounds the evolved system υ Sgr, storing a considerable part of the lost material, a substantial part of the Hα, Hβ, and the HeI 6678 Å line emission derives from regions perpendicular to the orbital plane of β Lyr.

Key words. stars: emission-line, Be – binaries: close – circumstellar matter – stars: mass-loss – stars: individual: β Lyrae – stars: individual: υ Sagittarii

1. Introduction

Mass loss and mass transfer in the evolution of close binary systems as well as the nature of some of the observed variations are unsolved problems (Harmanec 2002). With the exception of eclipsing binaries, the presence of the circumstellar structures and circumbinary envelopes is mainly deduced from the often ambiguous transformation from the velocity into cartesian space. From this point of view, interferometry or, even more, spectro-interferometry can bring new insights into these complicated systems, permitting direct access to the spatial information of the circumstellar structures. This paper reports on VEGA/CHARA spectro-interferometric observations in the visible of the famous massive interacting binary systems υ Sagitarii and β Lyrae.

The eclipsing binary β Lyr (HD 174638, HR 7106, HIP 92420, $V = 3.4$–4.3 mag) is a nearly edge-on system involving an early B-type mass-gaining star embedded in an optically and geometrically thick disk that is accreting gas from a less massive late B6-B8 II Roche lobe filling mass-losing companion. Following De Greve & Linnell (1994), β Lyr is near the end of a non-conservative case B mass transfer.

Harmanec et al. (1996, hereafter HMB96) presented an interferometric and spectroscopic campaign performed in 1994 based on observations in the visible from the GI2T (Grand Interféromètre 2 Télescopes). These observations showed that the violet (V) and red (R) sides of the Hα and HeI 6678 Å line were both resolved with the 50 m north-south baseline and that no variation of the interferometric signal with the orbital phase was detected. Together with the analysis of the phase-locked

radial velocity (RV) variations of the emission lines interpreted by the authors as evidence that the Hα line, and probably also the HeI 6678 Å line, bulk emission originate from an extended jet-like region perpendicular to the orbital plane, with nearly north-south orientation.

This bipolar flow was then confirmed by Hoffman et al. (1998, hereafter HNF98) based on an extended set of spectropolarimetric observations in the UV and in the visible, with a resolving power sufficient to isolate some strong lines such as Hα, Hβ, HeI 5876 Å or HeI 6678 Å . They proposed a detailed model in which the UV continuum originates from the accretion disk, and is scattered by the bipolar outflow, the Hα and Hβ being emitted mainly in the polar flow, despite a significant contribution from the equatorial environment and the hot spot, and the HeI 6678 Å originates from the mass flow between the gainer and the donor. The material possibly connected with the bipolar flow is also inferred by the resolved radio nebula observed around β Lyr (Umana et al. 2000, 2002). An extensive spectroscopic and photometric study (Ak et al. 2007) has given new support to the presence of a thick disk and bipolar jets in this system. The first resolved images of the eclipsing binary β Lyr were obtained from near-IR observations with the CHARA interferometer and the MIRC combiner (Zhao et al. 2008). Image reconstruction and model fitting were used to improve the parameters of the visual orbit to an unprecedented accuracy. The estimate of the position angle of the ascending node Ω is almost perpendicular to the orientation of the jet (~164°) inferred by HNF98. The distance $d = 314 \pm 17$ pc estimated by combining the semimajor axis with the spectroscopic linear separation $a \sin i$ is consistent with the revised Hipparcos distance $d = 296 \pm 16$ pc (van Leeuwen 2007). No evidence of bipolar emission is detected from these continuum H-band observations. Despite this recent progress, the mechanism of mass exchange and the physics of the mass-ejection from the equatorial plane remains to be better constrained. We need to improve our knowledge of the location and the morphology of the different line-forming regions that trace different components of the system. NPOI interferometric observations in the visible (Schmitt et al. 2009, hereafter SPT09) with limited spectral resolution show an extension of the Hα line forming region and also provide some constraints on the position angle of the line of node of the Hα.

The evolved system υ Sgr (HD 181615, HR 7342, HIP 95176, $V = 4.61$ mag) includes an A-type low-mass supergiant, which is the brightest member of the type of extremely hydrogen-deficient binaries stars (HdB stars). Some evolutionary scenarios for υ Sgr as a HdB star were presented by Schönberner & Drilling (1983) and by Eggleton (2002), in which this system is in a second phase of mass transfer where the primary has ended the core helium burning phase.

υ Sgr has long been known as a single-lined spectroscopic binary ($P = 137.9$ d). The secondary orbit was determined by the cross-correlation technique applied to the IUE spectra (Dudley & Jeffery 1990). The secondary ("invisible") component seems to be more massive ($q = 1.59$). However, the detection of the secondary lines is uncertain given the low SNR of the IUE spectra and requires an independent verification. This implies that the primary, defined on the basis of its relative brightness in the visible, could also be called secondary on the basis of its mass. We adopt for the remainder of this paper the identification proposed in Koubský et al. (2006, hereafter KHY), calling the star that dominates the visible *star_1* and the faint or hidden secondary *star_2*.

Nariai (1967) proposed that the blue-shifted Hα absorption is formed in a supersonic flow generated as the gas is transferred from the primary via the L1 point toward the secondary and escapes from the system as an outflowing spiral arm encircling the whole binary. The peculiar RV curve of the blue-shifted Hα absorption lead KHY to propose an alternative model: υ Sgr might be a non-eclipsing analog of the β Lyr system, provided that the peculiar spectrum of *star_1* would come from the inner rim of an inclined disk, while the blue-shifted absorption would originate from a slowly precessing bipolar jet.

The circumbinary material is also detected from the strong infrared excess of υ Sgr. Recent optical interferometry observations in the mid-IR reported by Netolický et al. (2009, hereafter NBC) demonstrated that the dust is confined to a dense optically thick disk, with a small aperture angle (Wolf et al. 1999). The inner rim of the dusty disk is about 20 mas, i.e. 12 AU assuming $d = 595^{+94}_{-72}$ pc (van Leeuwen 2007). This discovery has improved the constraints on the inclination angle, now estimated to be $i = 50^{\circ}{}^{+10^{\circ}}_{-20^{\circ}}$). Based on this inclination estimate, the current mass of the two stars may be larger than 10 solar masses[1].

The VEGA recombiner of the CHARA (Mourard et al. 2009) array is a recently commissioned facility that provides spectrally dispersed interferometric observables, with a spectral resolution reaching $R = 30\,000$, and a spatial resolution of less than one mas in the visible. This instrument is particularly well suited to the study of the extended forming regions, and in particular Hα, as shown in (Rousselet-Perraut et al. 2010; Chesneau et al. 2010).

β Lyr was observed with an effective spectral resolution of $R \approx 1600$ and with projected baselines of about 34 m and 58 m. The scheme of these observations follows the strategy reported by Harmanec et al. (1996), because the S1S2 34 m baseline of CHARA is almost parallel to the 50 m baseline of the GI2T, in the direction of the bipolar outflow. For υ Sgr, the interferometric observations, including a study of the Hα line at effective spectral resolution $R \approx 400$, was obtained with projected baselines reaching 107 m. This angular scale allows us to probe the core of the system, because the estimated separation of the components is about 1–2 mas.

This paper is structured as follows. In Sect. 2 we present the observations and the data processing. The next two sections are devoted to the results and the constraints provided by the differential visibility through the emission-lines forming regions of β Lyr (Sect. 3) and υ Sgr (Sect. 4). A general discussion about the very large Hα forming region detected by interferometric observations for the two systems is given in Sect. 5. Some conclusion and perspectives are given in Sect. 6.

2. Observations and data processing

2.1. VEGA observations and data processing

The interferometric observations presented here were made with the Visible spEctroGraph And polarimeter (VEGA, Mourard et al. 2009), which is set up on the CHARA array located at the Mount Wilson Observatory (California, USA, ten Brummelaar et al. 2005). The observations proceeded during two different runs in August 2008 and July 2009. The red and blue detectors were centered around 660 nm and 490 nm, respectively, with the medium resolution setting ($R = 5000$). This provides simultaneous recording of data around Hα and HeI 6678 Å lines on the

[1] Although this estimate depends significantly on the analysis of the noisy IUE data.

Table 1. Journal of interferometric observations for υ Sgr and β Lyr.

Date	UT [h:mn]	JD 2 450 000+	Orbital Phase[a]	Base	Projected baseline Length [m]	PA [deg]	Calibrators[b]
β Lyr							
2008/07/30	04:48	4677.7003	0.496	S1S2	34.07	2.6	γ Lyr
2008/08/03	04:51	4681.7024	0.805	S1S2	34.07	−0.04	γ Lyr
2008/08/05	06:55	4683.7882	0.963	S1S2	34.01	−18.0	γ Lyr
″	09:20	4683.8889	0.971	S1S2	32.62	−33.5	γ Lyr
2008/08/08	07:15	4686.8024	0.199	S1S2	33.90	−22.0	γ Lyr
″	07:54	4686.8292	0.201	S1S2	33.65	−26.4	γ Lyr
2009/07/25	04:34	5037.6904	0.312	S1S2	34.08	6.6	γ Lyr
″	08:59	5037.8745	0.326	S1S2	33.51	−28.0	γ Lyr
2009/07/26	09:20	5038.8891	0.404	E1E2	58.62	−156.0	γ Lyr
υ Sgr							
2008/08/03	06:34	4681.7736	0.058	S1S2	23.0	−16.4	γ Sct, ν Cap
	07:48	4681.8250	″	W1W2	106.7	96.8	γ Sct, ν Cap
2008/08/07	06:12	4685.7583	0.087	S1S2	22.7	−14.5	γ Sct, ν Cap
2008/08/08	04:38	4686.6930	0.093	W1W2	91.5	84.8	γ Sct
	05:23	4686.7243	″	W1W2	100.7	88.2	γ Sct
2009/07/27	04:25	5039.6840	0.653	S1S2	22.8	+15.5	γ Sct
2009/07/27	07:24	5039.8083	″	S1S2	23.9	−21.1	γ Sct

Notes. [(a)] Computed orbital phase: for υ Sgr from KHY, Eq. (1); for β Lyr from Ak et al. (2007), Eq. (2). [(b)] Calibrator angular diameters (mas): γ Sgr (HD170296) = 0.44 ± 0.03; ν Cap (HD 193432) = 0.30 ± 0.02 from SearchCal@JMMC; γ Lyr = 0.742 ± 0.097 from Legett et al. (1986).

red detector and around Hβ lines on the blue one[2]. For each observation, VEGA recombined two of the six 1-m telescopes of the CHARA array. Details of the observations of β Lyr and υ Sgr can be found in Table 1.

During the observations of β Lyr, the S1S2 baseline was nearly perpendicular to the orbital plane of β Lyr and the projection of the baseline onto the sky did not vary much during the night. The position angle of the E1E2 projected baseline was about at 50° of the orbital plan direction. This is an advantage in the context of observations aimed at studying the jet-like line-forming regions. In 2008 useful data could be simultaneously recorded in good atmospheric conditions with the red and the blue cameras on the best nights (2008/07/30, 2008/08/05 and 2008/08/08) but only with the red camera for the night 2008/07/03. In 2009 the poor seeing conditions only permitted recording data with the red camera during the nights 2009/07/25 and 2009/07/26. The observations of β Lyr were interleaved with observations of the nearby calibrator star γ Lyr (HD 176437, V = 3.24 mag, B9III) on each night. For the angular diameter of γ Lyr we adopted $_{\rm ld}$ = 0.742 ± 0.097 mas from Leggett et al. (1986). This limb-darkened disk diameter was converted to uniform disk diameters using $T_{\rm eff}$ = 10 005 K and log g = 2.91 from (Huang & Gies 2008) and linear limb-darkening coefficients computed by Diaz-Cordoves et al. (1995): $_{\rm ud}$[red] = 0.718 ± 0.094 mas and $_{\rm ud}$[blue] = 0.707 ± 0.093 mas.

The magnitude of υ Sgr (V = 4.6 mag) and its low declination (δ = −16°) strongly limits the signal-to-noise ratio at medium resolution because of the high airmass, and restricts the observability to about 4 h at most under good atmospheric conditions and the uv coverage. The observations of υ Sgr were interleaved with observations of the nearby calibrator stars γ Sct (HD 170 296, V = 4.68 mag, A1 IV/V, $_{\rm ud}$[red] = 0.43 ± 0.03 mas and $_{\rm ud}$[blue] = 0.42 ± 0.03 mas) and ν Cap (HD 193432, V = 4.75 mag, B9IV, $_{\rm ud}$[red] = 0.29 ± 0.02 mas and $_{\rm ud}$[blue] = 0.28 ± 0.02 mas) selected with the SearchCal[3] tool (Bonneau et al. 2006).

The data reduction is extensively described in Mourard et al. (2009) and we here briefly summarize the applied treatments.

2.1.1. Spectra

The spectra were extracted using the classical scheme: integration of the 2D flux in one spectrum, wavelength calibration using a Th-Ar lamp and normalization of the continuum by polynomial fitting.

Owing to an improved instrumental sensitivity in 2009, neutral density filters of 0.3 mag were systematically used for observing β Lyr. Spectra with a resolution of R = 5000 and S/N of 300−350 were obtained. The accuracy of the wavelength calibration was checked by performing a Gaussian fit to the core of the Hα line of the calibrator, γ Lyr. The standard deviation is 27 km s^{-1}, corresponding approximatively to one pixel on the detector in the medium spectral resolution mode (R = 5000). For β Lyrae, the values of the ratio of the peak intensity in Hα to the continuum intensity systematically appear to be about 33% lower than the expected value at the same orbital phase taken from Fig. 5 in (Harmanec et al. 1996) or Fig. 12 in (Ak et al. 2007). The difference mainly originates from a saturation effect of the photon-counting camera in the emission line. After careful testing, we found that the saturation does not affect the interferometric measurements (Delaa et al. 2011).

In the case of υ Sgr 30 000 short-exposure (15 ms) frames were typically recorded, providing a signal-to-noise ratio of 350−400 per spectrum. Two spectra containing the Hα line, obtained in the 2008 (orbital phase ϕ = 0.05) and 2009 (ϕ = 0.65) runs are presented in Fig. 1. In the figure the spectra are corrected from the saturation effect by increasing the line flux relative to the continuum by 40%, in agreement with the spectrum published in KHY. No Hβ line is observed in the blue camera,

[2] Note that for υ Sgr almost no strong hydrogen line is detected apart from Hα.

[3] http://www.jmmc.fr/searchcal/

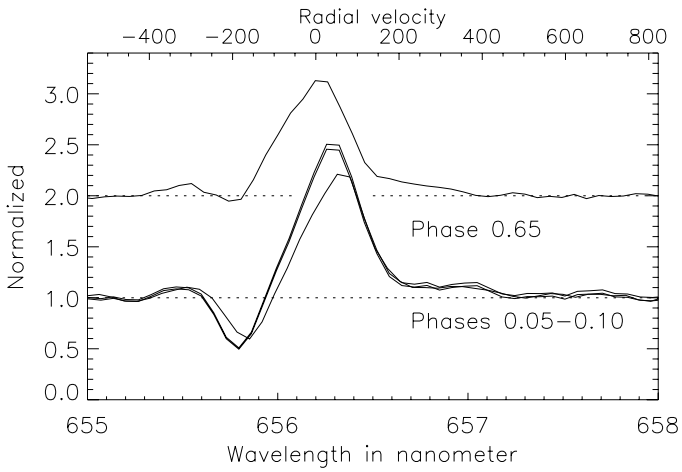

Fig. 1. Hα profiles of υ Sgr as measured by the VEGA spectrograph (R = 5000). The shape of the lines recorded in 2008 looks very similar to the 2005 ones for phase 0−0.1 (Koubský et al. 2006).

which is indicative of the pronounced hydrogen deficiency of the primary star.

2.1.2. Calibrated visibilities

The raw squared visibilities (V^2 measurements) are estimated by computing the ratio of the high-frequency energy and the low-frequency energy of the averaged spectral density of the frames. A selection process based on the statistics of short sequence measurements as well as visual inspection of the quality of the fringe signal was made. Calibrated squared visibilities were obtained by using the raw measurements of the calibrator star and its expected V^2 was calculated with its angular diameter estimate and the observing parameters.

For υ Sgr, the computations of V^2 were performed using different spectral windows; one window on the "reddest" side of the blue camera (λ_0 = 520 nm, $\Delta\lambda$ = 13 nm), and different windows with the red camera (λ_0 = 641 nm, $\Delta\lambda$ = 18 nm; λ_0 = 656 nm, $\Delta\lambda$ = 18 nm; λ_0 = 666 nm, $\Delta\lambda$ = 13 nm). The calibrated squared visibilities V^2 are given in Table 4. For the W1W2 baseline, only the red detector data were good enough to obtain reliable measurements. The squared visibilities measured with the S1S2 baselines show that the source is significantly resolved. The squared visibilities recorded with the W1W2 baseline were only slightly lower than those from S1S2 baseline. No significant change of the squared visibilities were observed among the different windows chosen within the red band. A change of the value of the squared visibility was observed between the blue and red cameras, albeit with a weak significance given the level of errors. The squared visibilities also seemed constant with time, because no significant differences are observed between the 2008 and 2009 data.

2.1.3. Differential visibilities and phases

The interferometric information in a spectral line was extracted by computing differential quantities between a large reference channel centered in the continuum of the source and a sliding science narrow channel, using the so-called cross-spectrum method (see Mourard et al. 2009, Sect. 3.4.2). At each wavelength analyzed by the narrow channel, the size of the source along the projected baseline can be estimated by measuring the modulus of the spectrally dispersed visibility $V(\lambda)$. Moreover, information related to the position of the photocenter of the source can be deduced by measuring the phase of the visibility $\varphi_{\rm diff}(\lambda)$ across a spectral line.

For the analysis of β Lyr observations, we used a science channel of 0.4 nm moving by steps of 0.4 nm so that the differential visibility is obtained with an effective spectral resolution of about 1650 around Hα line. For the four 2008 nights the rms of the spectrally dispersed visibility $V(\lambda)$ in the continuum reference channels is about 2−5% in the red (at λ647.0−665.0 nm and λ664.0−672.0 nm) and 5−10% in the blue (at λ481.5−490.7 nm) at visibility 1. The rms of the differential phase $\varphi_{\rm diff}(\lambda)$ is about 1.4–4.1° in the red and 4.2–6.2° in the blue. For nights 2009/07/25, the rms of $V(\lambda)$ is about 5−10% in the red continuum reference channels at visibility 1 and the rms of $\varphi_{\rm diff}(\lambda)$ is about 1.5–4.0°. For the night 2009/07/26, rms of $V(\lambda)$ is about 10−15% and the rms of $\varphi_{\rm diff}(\lambda)$ is about 3–5°. Figures 2–4 illustrate the best observations of β Lyr secured in 2008 and 2009.

For υ Sgr, we used a science channel of 1.4 nm moving by steps of 0.7 nm as a consequence of the low signal-to-noise ratio, and Hα is the only line that can be studied in the visible spectrum. This corresponds to an effective spectral resolution of about 400, which forces us to consider the Hα line as a whole, which in turn smears the signal from interesting parts of the line such as the blue P-Cygni component.

υ Sgr exhibits a strong variation of the visibility in the Hα line for short and long baselines as well as a clear differential phase signal for the S1S2 baseline. For the W1W2 baseline, the differential measurements are not reliable owing to the low signal-to-noise ratio in the line. The residual noise on the phase measurements is about 10°. The short baseline phases exhibit a clear and changing offset compared to the continuum. Interestingly is that the sign of the differential phases is inverted between orbital phase 0 and 0.6.

One can improve upon this analysis by performing an estimation of the intrinsic visibility $V_{\rm emi}$ of the source emitting the line by removing the continuum signal $V_{\rm cnt}$ from the observed signal $V_{\rm obs}$ using the relation:

$$V_{\rm emi} = (V_{\rm obs} - C_{\rm cnt} V_{\rm cnt})/(1 - C_{\rm cnt}). \quad (1)$$

$C_{\rm cnt}$ is the relative contribution to the total flux of the underlying continuum source in the spectral channel. If the spectral resolution is such that the line is not resolved, $C_{\rm cnt}$ can be derived from the measurement of the equivalent width (EW) of the emission line, if possible corrected for an underlying photospheric absorption. If the line is resolved, one can perform an estimation of $C_{\rm cnt}$ per spectral channel using measurements of the line-to-continuum ratio, taking into account, if possible, an underlying photospheric absorption.

3. Results on β Lyr

For the observations of β Lyr carried out with the S1S2 baseline, the V^2 measurements in the continuum give values of V^2 = 1.00 ± 0.15 in 2008, and V^2 = 0.90 ± 0.10 in 2009. β Lyr is found to be nearly unresolved as expected from the short baseline length and the orientation baselines perpendicular to the orbit on the sky. We used a toy model of the system to evaluate the level of visibilities. The toy model consists only of two nearly unresolved sources, with the orbital parameters based on the parameters from Zhao et al. (2008), and the flux ratio in the visible between the components from Schmitt et al. (2009). The expected values of V^2 are ≤0.90 and ≤0.86, in the red and

Table 2. β Lyrae calibrated visibility and differential phase in the spectral lines Hα, Hβ, HeI 6678 Å .

	Line parameters				Interferometric parameters		
Orbital phase	W [Å]	V peak [km s^{-1}]	Abs.Comp. [km s^{-1}]	R peak [km s^{-1}]	Vmin	Center [km s^{-1}]	$\phi_{\rm diff}$ [deg]
			Hα line				
0.199	−8.0[a]	−183	−98	123	0.73 ± 0.03	−49	+8 ± 2
0.201	−8.0[a]	−185	−88	116	0.73 ± 0.03	−49	+10 ± 2
0.312	−12.7[a]	−135	−57	98	0.73 ± 0.08	−100	+15 ± 5
0.326	−14.4[a]	−147	−73	122	0.79 ± 0.05	−102	−5 ± 5
0.404	−13.5[a]	−157	–	80	0.62 ± 0.12	−2	25 ± 9
0.496	−16.4[a]	−74	10	200	0.65 ± 0.02	57	−10 ± 2
0.805	−10.8[a]	−153	−64	133	0.73 ± 0.05	45	15 ± 4
0.963	−23.6[a]	−170	−115	67	0.58 ± 0.03	8	12 ± 3
0.971	−23.6[a]	−164	−177	75	0.67 ± 0.05	10	+18 ± 3
			Hβ line				
0.199	0.0[b]	−180	−173	208	0.79 ± 0.08	–	−19 ± 5
0.201	0.0[b]	−184	−171	210	0.80 ± 0.09	–	−17 ± 8
0.496	−0.18[b]	−84	14	200	0.71 ± 0.05	–	0 ± 7
0.971	−0.3[b]	−170	−32	111	0.66 ± 0.10	–	+22 ± 5
			HeI 6678 Å line				
0.199	−1.1[c]	−210	−63	204	0.79 ± 0.03	20	+7±2
0.201	−1.1[c]	−213	−62	202	0.80 ± 0.03	−27	0±2
0.312	−1.1[c]	–	–	–	0.93 ± 0.05	–	0 ± 3
0.326	−1.1[c]	–	–	–	1.00 ± 0.06	–	0 ± 3
0.404	−1.2[c]	–	–	–	0.78 ± 0.08	–	+15 ± 5
0.496	−4.7[c]	−87	56	76	0.74 ± 0.04	66	0 ± 2
0.963	−2.2[c]	−130	−55	106	0.71 ± 0.05	17	0 ± 2
0.971	−2.2[c]	–	–	–	0.51 ± 0.08	47	+22 ± 4

Notes. [(a)] Multiplied by 1.33 to correct for the saturation of the line. A value of 8 Å can be added to take into account a realistic absorption component. [(b)] A value of 6 Å can be added to take into account a realistic absorption component. [(c)] This estimate was multiplied by 1.2 to correct for the saturation of the line.

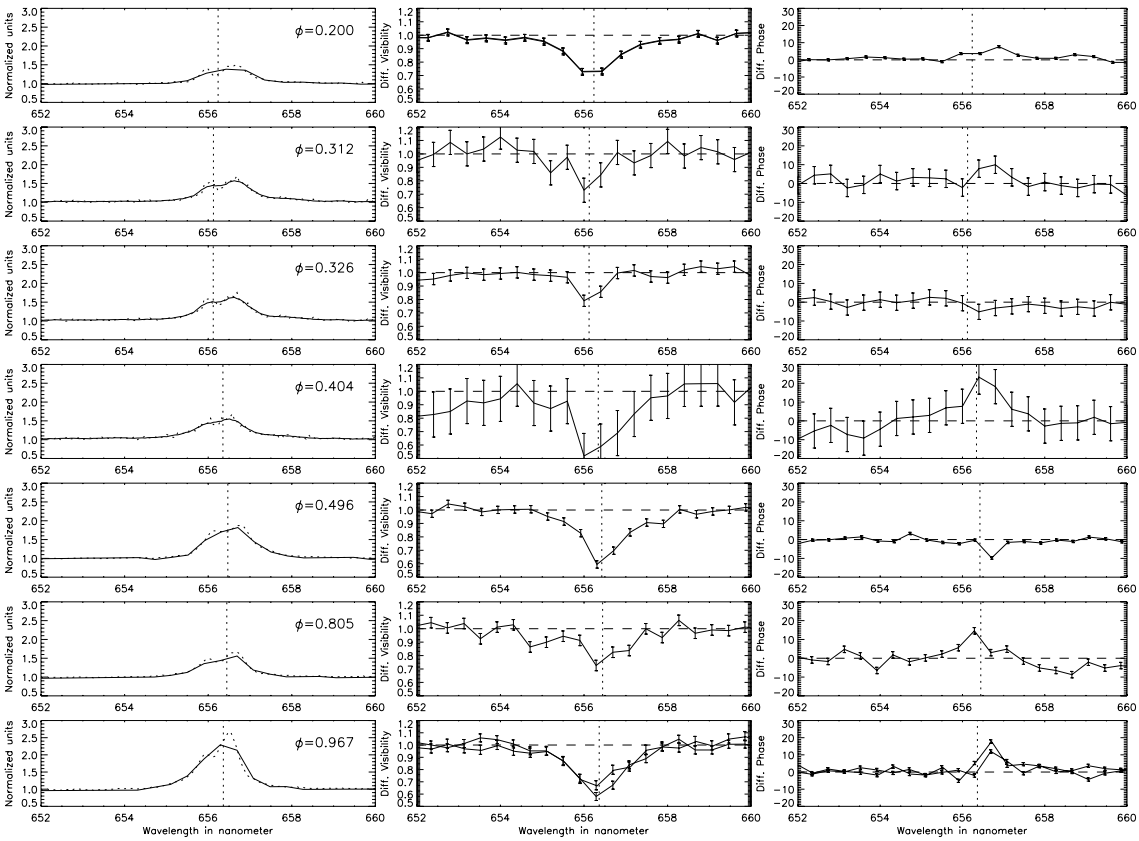

Fig. 2. 2008 and 2009 observations of β Lyr in Hα. *Left*: spectrum around Hα line with $R = 5000$ (dotted line) and binned flux at $R \approx 1650$ (line). Differential visibility normalized to the continuum (*center*) and the differential phase (*right*).

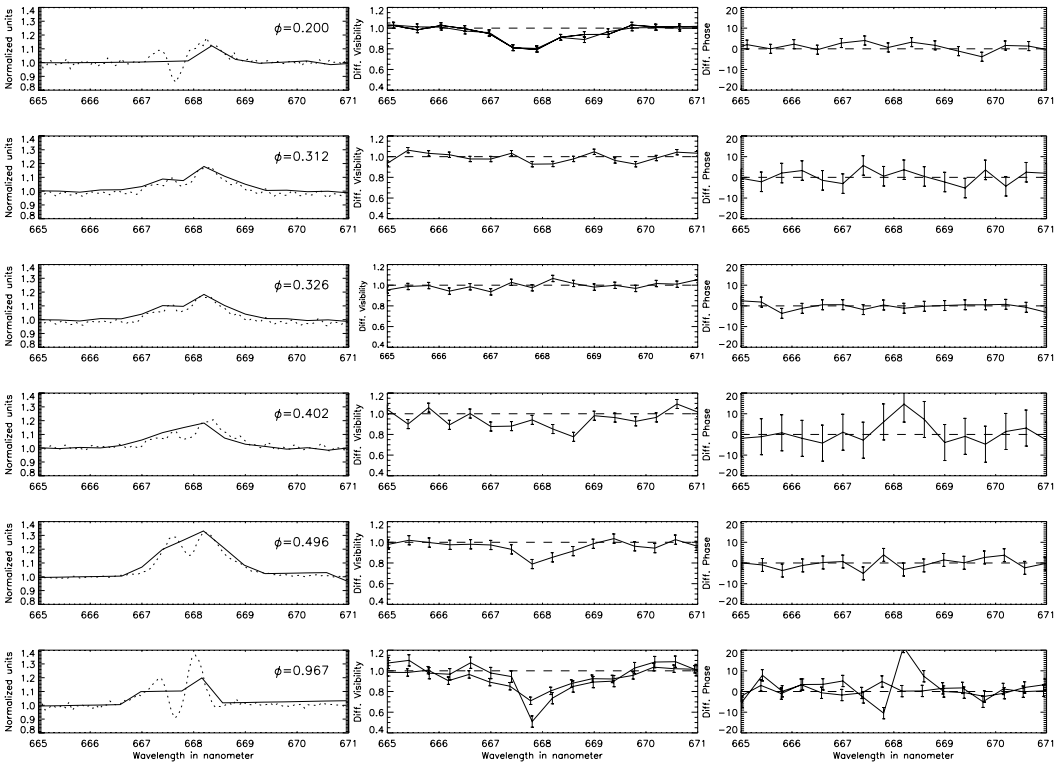

Fig. 3. Observation of β Lyr around the HeI 6678 Å line. *Left*: spectrum with $R = 5000$ (dashed line) and binned flux at $R \approx 1650$ (solid line). Differential visibility normalized to the continuum (*center*) and the differential phase (*right*).

blue continuum, respectively. At any orbital phase, the source visibility in the continuum can be taken to be $V_{\rm cnt} \approx 1.0$, and we will not be comment on this further. For the E1E2 baseline observations (26th of July 2009), the measurements provide a value of $V^2 = 0,73 \pm 0,10$ in agreement with the expected value from the toy model. For this last measurement the hypothesis of an unresolved continuum is no longer valid, and the continuum visibility was taken into account when computing angular extension estimates from Eq. (1).

3.1. The line-forming regions in the β Lyr system

Some preliminary results can be inferred starting from the simple examination of Figs. 2–4. Evidently the dispersed visibilities in Hα, Hβ and HeI 6678 are all significantly decreased compared to the continuum level, indicating an environment more extended than the continuum in the direction of the projected baselines, which have an orientation generally nearly perpendicular to the orbital plane.

The β Lyrae calibrated visibility normalized to the continuum $V_{\rm cal}$ [line] and the differential phase $\varphi_{\rm diff}$ [line] are given in Table 2 as a function of the orbital phase $\phi_{\rm orb}$. We emphasize the high observed variability of the EW of the Balmer and Helium lines in the course of the orbital phase, which illustrates that the differential visibility measurements originate in a complex source that consists of a mix of continuum and line emission from various components, whose Doppler velocity and flux vary in the course of the orbit. Assuming a continuum at level 1 is probably not realistic for the computation of the EW, because the B6II primary star exhibits a deep Hα absorption line. We used the assumptions on the underlying absorption EW given and justified in Hoffman et al. (1998, cf. Tables 5 and 6) of 8 Å and 6 Å for the Hα and Hβ line, respectively. No such correction was applied to the EWs from the helium lines.

The spectral resolution of the VEGA interferometric data is sufficient to resolve the line, and the line-to-continuum ratio at the minimum visibility is a good estimate to use in Eq. (1). An estimate of the extension of the source associated with the emission line was obtained by computing the $FWHM$ of a Gaussian disk model. The results of this analysis are given in Table 3.

The difficulty of this calculation is to use the best estimate of the line-to-continuum-flux ratio $C_{\rm cnt}$, especially for a source as complex as β Lyr. For instance, taking into account this absorption, the fractional contribution of the continuum in the bandwidth of the NPOI Hα channel (15 ± 1 nm) ranges from 83% to 91%, and it is probable that during the primary eclipse this percentage is even lower. This contributes to the difficulty in infering an unbiased orbit of the Hα emission as discussed in Schmitt et al. (2009). In the VEGA context of a spectrally resolved line, we measured the Doppler position of the deepest level of the differential visibility in the line. This observable is affected in a complex manner by the absorption component that is locked to the orbital motion of the primary and affects the Hα line within a narrow range of velocities. A consistent investigation of the Hα line forming system requires an in-depth study of the physical parameters of the different emitting regions and their kinematics, and such a detailed analysis requires the developement of a consistent model which is beyond the scope of the paper.

3.1.1. The Hα line

The source associated with the Hα line is significantly resolved at each orbital phase. These measurements qualitatively agree with the GI2T and NPOI measurements, although the effect of the different spectral resolution must be carefully taken into account. For instance, the mean of the VEGA S1S2 visibilities in

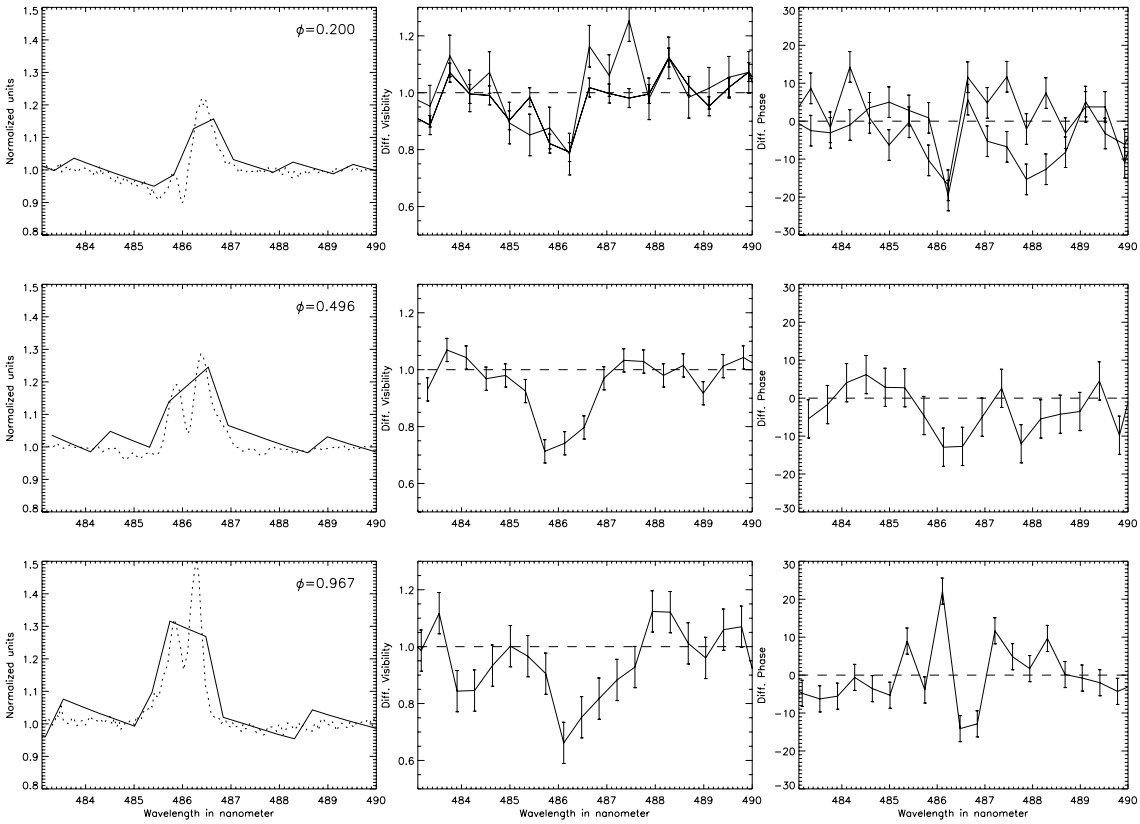

Fig. 4. 2008 observations of β Lyr in Hβ. *Left*: spectrum around Hβ line with $R = 5000$ (doted line) and binned flux at $R \approx 1650$ (line). Differential visibility normalized to the continuum (*center*) and the differential phase (*right*).

Table 3. Estimates of the angular extend of β Lyrae in the Hα emission line at the orbital phase of the observations.

Orbital Phase	f [M_λ]	$C_{\rm cnt}$	$V_{\rm emi}$	Err$V_{\rm emi}$	$_{\rm emi}$ [mas]	Err$_{\rm emi}$ [mas]
0.199	51.7	0.57	0.38	0.07	2.10	0.22
0.201	51.3	0.57	0.37	0.07	2.12	0.20
0.312	51.9	0.53	0.43	0.17	1.94	0.47
0.326	51.1	0.50	0.58	0.10	1.59	0.25
0.404	89.4	0.61	0.03	0.30	2.32	1.00
0.496	51.9	0.43	0.38	0.04	2.07	0.10
0.805	51.9	0.52	0.43	0.10	1.94	0.28
0.963	51.8	0.33	0.38	0.05	2.09	0.13
0.971	49.7	0.32	0.51	0.07	1.80	0.19

Notes. The columns give the spatial frequency $f = B/\lambda$, the relative contribution of the continuum flux C_{cnt} , the estimate of intrinsic visibility of the emitting source $V_{\rm emi}$ and $_{\rm emi}$ the $FWHM$ of a Gaussian disk model. The scale is about 0.3 AU per mas.

the core of the line is 0.70 and the standard deviation (rms) is 0.08. This is twice as high as the typical error bar and is an indication of orbital variability. Using the continuum corrected estimates of the equivalent $FWHM$ reported in Table 3, we found a simple mean $FWHM$ of 1.99 ± 0.20 mas. A weighted mean, that accounts for the highly variable error bars provides an estimate of 2.05 ± 0.20 mas.

The largest extensions are found at the primary and secondary eclipses. Outside the eclipses, the mean visibility is 0.75 ± 0.03, an rms equivalent to the error bar of the individual measurements. The slightly lower visibilities at the eclipses can be explained by the disappearance of a compact component contributing to the Hα emission. At phase 0, this is the eclipse of the primary, which is heightened by the Hα self-absorption of the disk. At phase 0.5 the accretion disk is eclipsed. A parallel can be found with the qualitative interpretation of the spectropolarimetric data recently proposed by Lomax & Hoffman (2011).

These results roughly agree with the GI2T (HMB96) and NPOI (SPT09) observations. Three kinds of differential visibility measurements were presented in HMB96 using the 50 m north-south GI2T baseline: a mean visibility of the whole line of 0.55 ± 0.13, a visibility of the V peak of 0.39 ± 0.12 and a higher visibility of the R peak 0.59 ± 0.15. With the greater spectral resolution of the VEGA data, one can directly see in Fig. 5 that the dip of the differential visibilities is located close to the V peak during the second half of the orbital phase, and closer to the radial velocity of the absorption component in the first half. The NPOI measurements, including a continuum flux correction (constant over the orbital phase), suggest a smaller $FWHM$ of 1.2 mas. We note that the longest NPOI baselines probed essentially the east-west direction, perpendicular to the outflow. These baselines have a large weight for the fitting procedure. This may suggest a limited opening angle for the jet, but we refrain to elaborate further on this because of to the large differences in terms of spectral resolution and uv coverage between the two arrays and instruments, and the complexity of the source.

3.1.2. The Hβ line

The quality of the Hβ signal, despite being much lower than for the Hα line in the red, is consistent with the results found in the previous section. A good signal could not be retrieved at all dates of observation, but one can see that the visibilities in the line at phase 0.2 are higher compared to those obtained during the

Table 4. Results of υ Sgr interferometric observations.

Date	UT	Projected baseline		Absolute visibilities			Differential observables	
	[h:mn]	length [m]	PA [deg]	$V^2_{0.52\ \mu m}$	$V^2_{0.64\ \mu m}$	$V^2_{0.67\ \mu m}$	$V_{H\alpha}$ [deg]	$\phi_{H\alpha}$
2008/08/03	06:34	23.0	−16.5	0.68 ± 0.19	0.66 ± 0.11	0.71 ± 0.11	0.41 ±0.09	28±10
	07:48	106.7	96.8	–	0.87 ± 0.11	0.68 ± 0.20	0.38 ± 0.10	36 ± 20[a]
2008/08/07	06:12	22.7	−14.5	0.71 ± 0.08	0.81 ± 0.08	0.68 ± 0.07	0.27 ± 0.06	46 ± 10
2008/08/08	04:38	91.5	84.8	–	0.62 ± 0.08	0.70 ± 0.08	–	–
	05:23	100.7	88.2	–	0.51 ± 0.08	0.62 ± 0.05	–	–
2009/07/27	04:25	22.8	+15.5	0.73 ± 0.15	0.79 ± 0.06	0.88 ± 0.07	0.46 ± 0.07	−2 ± 5[a]
2009/07/27	07:24	23.9	−21.0	0.72 ± 0.1	0.93 ± 0.08	0.82 ± 0.05	0.51 ± 0.08	−25±6[a]

Notes. [(a)] These results were obtained with an increased bin size (see text).

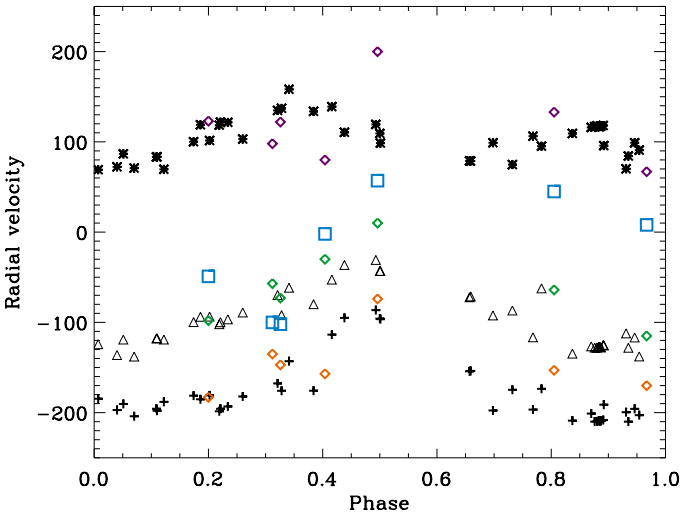

Fig. 5. Radial velocities of the V (violet diamonds) and R peaks (red diamonds), the absorption component (green diamonds) and the dip of the differential visibilities (blue squares) in the Hα line. The Harmanec et al. (1996) velocities are shown for comparison (V peaks represented by stars, R peaks by crosses and absorption components by triangles).

eclipses at phases 0.496 and 0.971. The Hβ line forming region is extended, ranging from a $FWHM$ of 1.5 mas to more than 2.0 mas during the primary eclipse. These results are in line with the results from Hα, and Hα and Hβ are treated in a similar way in the interpretation of Hoffman et al. (1998).

3.1.3. The helium line

The HeI 6678 Å exhibits a profile intermediate between Hα and Hβ in the sense that the absorption component is deeper than Hα but less pronounced than Hβ. The source is resolved at all orbital phases and no clear differential phase is detected. The mean visibility is 0.71 and the rms of the measurements is 0.12. Again, the lowest visibilities are observed near the eclipses. These visibilities show that the HeI 6678 Å line-forming region is at least as extended as the Hα one, reaching a $FWHM = 2$ mas and probably even higher considering that the equivalent width of the HeI 6678 Å line is much smaller. This large extension is remarkable. As discussed in HNF98, HeI 6678 Å is too far above the ground level to be collisionally excited and must arise from helium recombination within a hot medium. This is why they tentatively associated the HeI 6678 Å forming region to the mass-stream, although the hot spot and the jets might also reach the physical conditions for its emission. The estimated continuum-corrected $FWHM$s from the HeI 6678 Å are highly variable. This might reflect a larger error when performing the sensitive continuum correction, but it is striking to notice that the temporal behavior is fully consistent with the results from the Hα and Hβ lines, and might reflect a higher variability of the coherent flux from this line, related to the physical constraints of its emission. The VEGA observations suggest that HeI 6678 Å is both formed in the extended outflow, facing an intense hard radiation, probably from the accretion disk and/or the hot spot. The hot spot also contributes significantly, which explains the small scales inferred between phases 0.3 and 0.4.

3.2. Parallel with spectropolarimetric observations

The time variability of the photometry and the spectroscopic information from the line (flux, Doppler velocities) was extensively used in the past to recover the complex geometry of this system (Ak et al. 2007, and references therein). This time monitoring was also performed using spectropolarimetry and provided interesting information that can be compared with the optical interferometry data, at least qualitatively (Lomax & Hoffman 2011, HNF98). The spectropolarimetric signature of the hot spot is a local depolarization of the line, whereas it is seen by the interferometer as a compact line source (i.e. with a high visibility). The depolarizing effect results in a temporal shift between the minimum visible flux and minimum of polarization at orbital phase 0.487, which provides a constraint on the maximum size of the hot spot, 25−30 $R_\odot$, i.e. 0.38−0.45 mas. One can wonder which is the best line to study the hot spot. The Hα line is used by Lomax & Hoffman (2011) and in HNF98 HeI 5876 Å HeI 7065 Å are suggested, while HeI 6678 Å is proposed to originate from the mass stream. We observed that the HeI 6678 Å estimated sizes are much smaller between phases 0.3 and 0.4, which points to a large contribution of the hot spot to the line emission at this orbital phase.

3.3. Summary

The observations of VEGA/CHARA provide elements that confirm the assumptions previously made on the morphology of the emission line forming regions. The findings are the following:

– The spatial extent of the Hα line appears to be different during and outside eclipses, showing that the line-forming regions consist of a compact source that is located in the vicinity of the orbital plane and probably associated with the hot spot, and a source extending above and below the orbital plane, the size of which can roughly be estimated by a

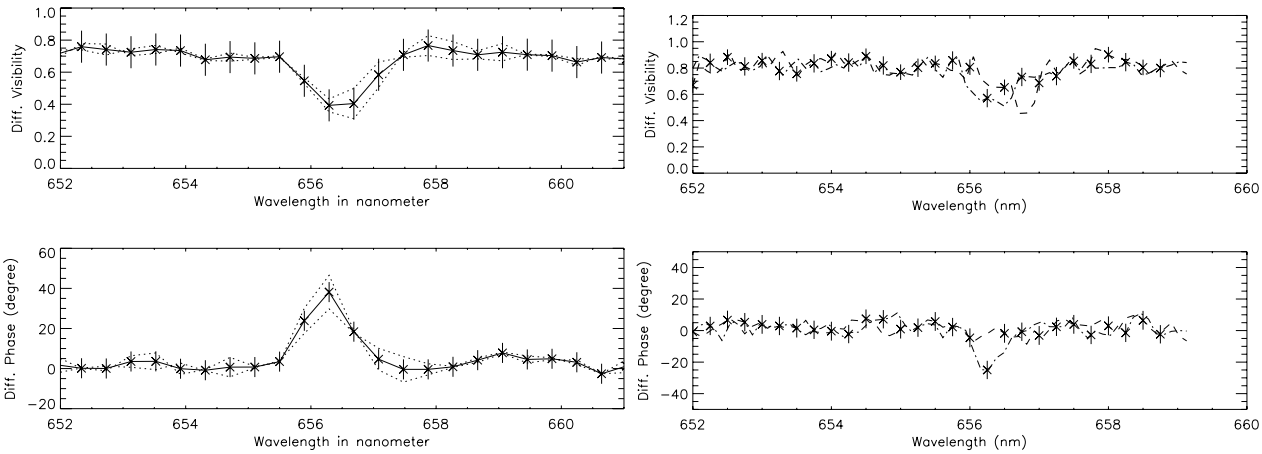

Fig. 6. S1S2 34m baseline differential visibilities and phases of υ Sgr through the Hα line in August 2008 at $\Phi_{\rm orb} = 0.06$ (*left*) and on 27th of July 2009 $\Phi_{\rm orb} = 0.65$ (*right*). The 2008 data recorded in five day intervals with similar projected baselines agree well within error bars (dotted lines). The bin size is 0.8 nm in 2008 and in 2009 (4 h 25 baseline: dashed line; 7 h 24 baseline: dash-dotted line). Note the opposite direction of the phase signal between the two epochs.

Gaussian distribution with a $FWHM$ larger than 2 mas. The Hβ line-forming region is less extended but follows a similar time-variation.

– The HeI 6678 Å line-forming region appears to be similar and at least as extended as the Hα one during the eclipses, while very small during phases 0.3–0.4. This suggests that the emitting regions could be an extended outflow that faces intense hard radiation sources from the accretion disk and the hot spot, in which favorable conditions for the emission of this line are encountered.

4. Results for υ Sgr

4.1. Interpretation of the continuum measurements

Several sources contribute to the continuum emission for the system in the visible (i.e. around 520 nm and 650 nm): the main part is from *star_1*, some is expected to come from the (hot) companion *star_2* and one may expect a contribution from the extended circumstellar environment. We first computed the expected configuration of the system at the time of the observation based on previous spectroscopic studies. We then conducted a fitting of the V^2 data under the assumption that the companion is not visible. Finally, we investigated whether or not a binary signal is present in the VEGA visibility-squared measurements.

4.1.1. Expected properties of the binary system

From the Hipparcos distance and the spectroscopic parameters of the system provided in KHY, one can estimate the amplitude of the interferometric signal and obtain some constraints for the observations. First, the radius of the circular orbit $A = 271^{+52}_{-31}\,R_\odot$ is obtained using Table 5 of KHY and the inclination $i = 50 \pm 10°$ derived from NBC. It provides an angular orbital radius $a = 2.1^{+0.4}_{-0.2}$ mas. The main axis of the system, inferred from polarimetric measurements (Yudin 2001) and VLTI interferometric measurements (NBC) is oriented at PA $= 80 \pm 10°$. Using the orbital parameters $P = 137.9343$ d, $T = 2\,433\,018.10$ $e = 0.0$ and $\omega = 0.0°$ from KHY and adopting from NBC the orientation parameters $i \approx 50°$ and $\Omega \approx 80°$, leads for 2008 and 2009 to the relative positions of the components given in Table 5 and to the visual configurations shown in Fig. 8. Second, the primary of the system *star_1* assumed to be an A0–B5 supergiant is in the range of 50–60 $R_\odot$ (Schönberner & Drilling 1983; Dudley & Jeffery 1990) although NBC estimated a radius of *star_1* from the luminosity estimate of 39 000 $L_\odot$. Using the Hipparcos distance, a $R_1 \approx 60\,R_\odot$ radius translates in an angular diameter of $\phi_1 \sim 0.8$–1.0 mas, well resolvable with VEGA/CHARA using a 90–110 m baseline (i.e. W1W2) at 650 nm, whereas a source as small as 10–15 $R_\odot$ (i.e. 0.15–0.27 mas) is virtually unresolved given the VEGA angular resolution. KHY estimated the Roche lobe diameter for the supergiant to be about 80–130 $R_\odot$, i.e. 1.1–2.1 mas (assuming an inclination $i = 50°$). The angular diameter of the hot companion is compact ($R_2 \approx 4\,R_\odot$ i.e. 0.05–0.07 mas) from Dudley & Jeffery (1990). The hot source cannot be resolved by VEGA/CHARA and its contribution can only be detected through a possible binary modulation of the visibilities, depending on the flux ratio of the components at 520 nm and 650 nm.

4.1.2. The best single-star geometrical interpretation

Despite the large range of baseline lengths, between 30 m and 100 m, no visibilities below 0.6 or above 0.9 were measured with VEGA. No uniform disk or Gaussian model can account for these data, and a realistic solution is to consider an extended source larger than 5 mas together with a compact stellar source. The presence of an extended emission is not surprising considering that the υ Sgr exhibits a large infrared excess that was spatially resolved using mid-IR interferometric observations from the VLTI (NBC). The mid-IR data were well-fitted by a model of a passive, vertically stratified disk whose estimated angular diameter of the inner rim must be fully resolved in the visible. This dusty disk can potentially be the origin of some scattered light. Moreover, significant emission is suspected from a disk of plasma located closer to the central source than the dust inner rim as shown by the Balmer lines in emission.

We performed a simple fitting process of the V^2 data using the `LITpro` software[4] (Tallon-Bosc et al. 2008). As discussed above, a uniform disk fails, providing a value of 2.04 mas with a $\chi^2 = 11.2$. A Gaussian disk model fails similarly with a $FWHM$ of 1.17 mas with $\chi^2 = 16.9$. We then included an extended component with the stellar source being described by a uniform disk. In model 1, the extended component is described by a Gaussian

[4] http://www.jmmc.fr/litpro_page.htm

Table 5. Configuration of υ Sgr system during VEGA observations.

Date	MJD 2 450 000+	Orbital Phase	θ (deg)	ρ (mas)
2008/08/03	4681.774	0.058	93.7	2.01
2008/08/07	4685.762	0.087	101.3	1.90
2008/08/08	4686.724	0.093	103.2	1.93
2009/07/27	5039.750	0.653	302.7	1.64

Notes. The scale is about 0.6 AU per mas.

Table 6. The best single-star geometrical model parameters for υ Sgr.

Model 1: $\chi^2 = 0.9$		
Parameter	Value	Error bar
star uniform diameter	0.37	0.21
star relative flux	85%	30%
Gaussian $FWHM$	≥5.9 mas	–
Gaussian relative flux	15%	8%
Model 2: $\chi^2 = 0.5$		
star uniform diameter	0.33	0.16
star relative flux	85%	30%
resolved component relative flux	15%	5%

of large $FWHM$. In model 2, the extended component is assumed to be completely resolved. The best-fit parameters are shown in Table 6.

At the distance of 520−690 pc, the angular diameter of 0.33 *mas* translates into a radius of ∼18−49 $R_\odot$. This is much smaller than the Roche-lobe radius estimates from KHY that range from 80 to 130 $R_\odot$, even considering a large uncertainty[5]. The primary can thus be considered as a hydrogen-deficient B8II-B5II supergiant. The fact that the primary star is far from filling its Roche-lobe implies that the accretion onto the hidden secondary, if this accretion is currently acting, must occur via a wind-capture.

4.1.3. Constraints on the binary signal

We have performed a computation of the expected signal using the observing configurations and the expected position of the components. The model consists of a primary described by a uniform disk with a diameter of 0.33 mas, an unresolved companion, and an extended component representing 15% of the total flux, as estimated in the previous section. Some examples with a flux ratio of 10 and 100 between the stellar components are shown in Fig. 7. These simulations indicate that the S1S2 baseline is not really sensitive to the binary signal and that a significant spectrally dispersed binary signal can be detected for W1W2 baselines between the red and blue cameras, and also within the red camera, provided that the separation is larger than 1 mas. The expected visibility differences between the W1W2 and S1S2 baselines are such that given the level of uncertainty of the V^2 measurements, we can reasonably exclude a binary signal with a flux ratio higher than 0.1. One can also see in Fig. 7 that significant differences between the S1S2 and W1W2 visibilities are expected with a flux ratio ten times higher.

No significant variation of the short and long baselines visibilities versus PA and time was detected with the 10–15% accuracy of the calibrated visibilities. It was not possible to measure sufficiently accurate calibrated visibilities in the blue with W1W2, which are clearly missing. The amount of data and the level of accuracy of the measurements shown in this study are not yet sufficient to provide stringent limits on a non-detection of the companion and an upper limit on the flux ratio between the components, and we refrain from attempting any fitting of the data within this context. The simulations shown here aim at suggesting that it is not unrealistic to consider that these constraints may be provided in the near future as a result of an ongoing observing campaign.

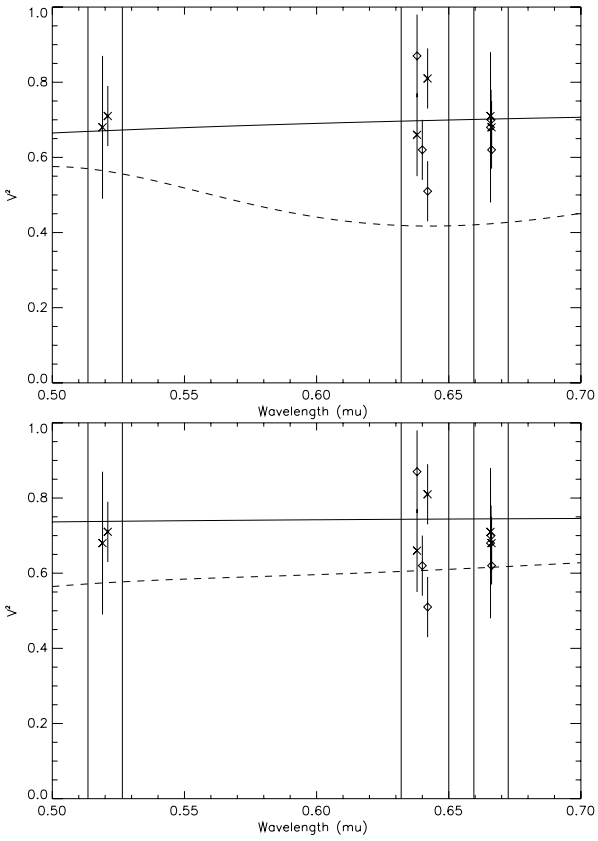

Fig. 7. Expected interferometric signal corresponding to the configuration of the system of υ Sgr during the 2008 interferometric observations applying the parameters from (Koubský et al. 2006; Netolický et al. 2009). *Upper panel*: the flux ratio of the component is 10. *Lower panel*: the flux ratio of the component is 100. The solid line represents the S1S2 short baseline and the dashed line the W1W2 long baseline. The vertical lines define the spectral bandpass used for the V^2 measurements described in Sect. 2.1.2. The measurements are shown as crosses with error bars (S1S2 measurements) and diamonds (W1W2 measurements).

The flux of the system is probably dominated by a single component with a flux ratio higher than 4–5. This result is in line with Dudley & Jeffery (1990), who also concluded that the luminosity ratio of the visible to "invisible" component must be about 100. One other possible explanation of our data is that the separation of the stars may have been much smaller than estimated. This hypothesis would imply that the distance of the system is greatly underestimated. In the absence of any pertinent criticism against the Hipparcos estimates, we shall consider this hypothesis as not probable.

4.2. Interpretation of the Hα line differential measurements

A rough orbital solution can be found for the Hα line in KHY. The Hα emission is located very close to the center of gravity of the system, at 0.13 AU only, in the direction of *star_1* but in fact

[5] That originate from the difficulty of inferring the orbit parameters of the secondary and therefore its nature.

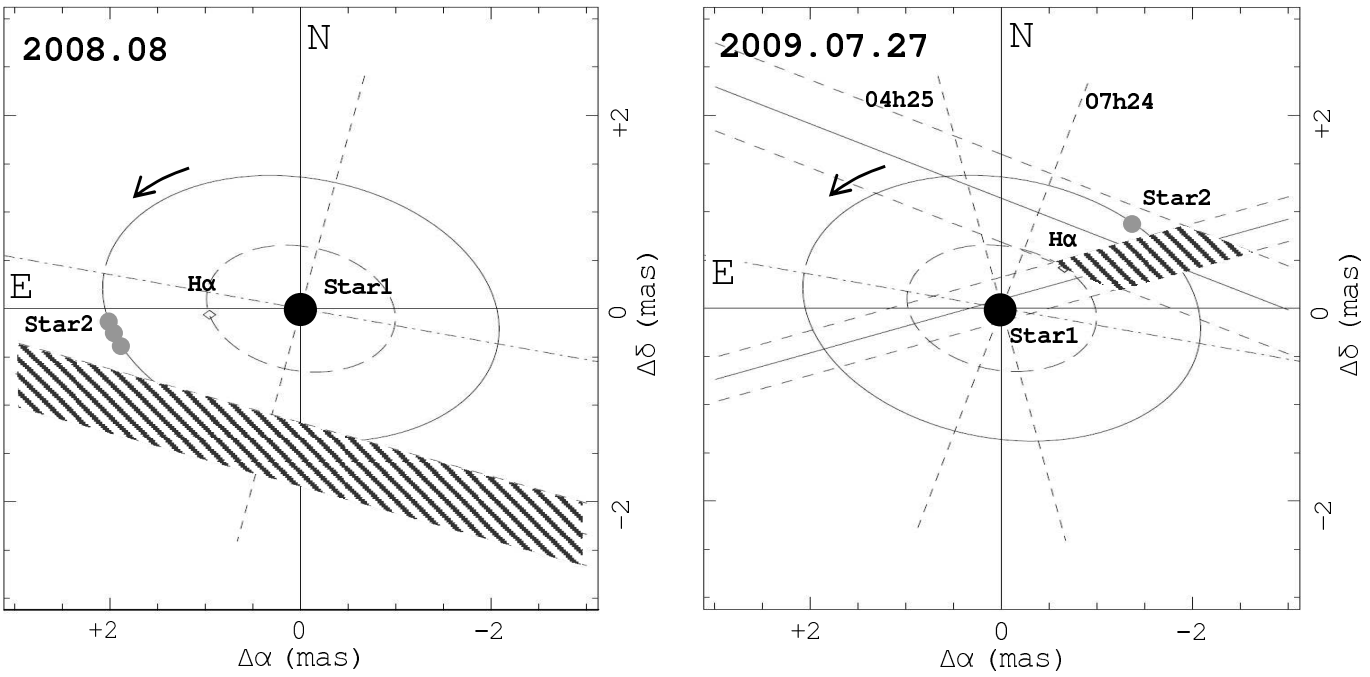

Fig. 8. Expected configuration of the υ Sgr system at the time of the interferometric observations compared with the best location of the bulk Hα photocenter inferred from the differential phase analysis. The visual orbit of the couple *star_1–star_2* is computed using the spectroscopic orbit of KHY and adopting the inclination and the position angle of the node from NBC. The orbit of the bulk of the Hα emission is shown following the spectroscopic orbit proposed by KHY. The S1S2 projected baselines at the time of the observations are also represented (dashed lines). The diagonal zones represent the constraints on the localization of the core of the Hα line imposed by the differential phase measurements. The hatched drawing zone for the 2009 observations takes into account the two measurements at different baseline orientations, while the single 2008 observation is not restrictive enough to provide tight constraints.

physically closer to *star_2* at 0.505 AU than *star_1* at 0.585 AU. The predicted position of the Hα emission is included in Fig. 8.

We note that at phase 0.65 (2009 observations) the differential phases are very different from one baseline to the other. Because the Hα emission is marginally resolved with the S1S2 baseline, we can interpret the measured differential phase signals as a photocenter displacement on the sky in the direction of the projected baseline. To extract the position of the emitting region from the photocenter position, we need to estimate the fraction of flux coming from the emitting region inside the considered spectral band. This is easily done from the binned spectral profiles and leads to the following values: 42% (resp. 37%) of the flux originates from the emitting region in 2008 (resp. 2009) in the spectral channels where the maximum phase signal is observed. We also make the assumption that the continuum emission (either from the primary star or the large surrounding nebula) shares the same photocenter and that the contribution of the secondary star is negligible within the error bars. The results are presented in Fig. 8 for the observations in 2008 and 2009 with the S1S2 baseline. The hatched drawing zones represent the expected localization of the Hα core emission.

These measurements suggest that the Hα is very close to the expected position of the "invisible" component *star_2*, and disagree with the orbital parameters proposed by KHY. The 2008 photocenter originates from a single measurement being the mean of two slightly disagreeing measurements, but the hatched area suggests that the photocenter of the Hα emission is close to the expected position of *star_2* at this epoch. The 2009 photocenter determined from two different projected baselines is more accurately defined, and clearly indicates that the photocenter of the Hα emission is not only located in the direction of *star_2*, but also in its vicinity.

The 2009 visibilities in the core of the Hα line from the two baselines are of similar depth, but are seen at slightly different wavelengths. This probably points to a complex spatial distribution and kinematics in the Hα line-forming region. NBY estimated the PA of the dusty disk to be 80^{+10}_{-5} degrees, i.e. perpendicular to the baseline oriented at $-21°$. In the case of υ Sgr, the intermediate inclination makes the Hα emission projected onto the sky by far less easily predictable than in the case of the interacting binary β Lyrae by Harmanec et al. (1996) seen at high inclination. It is also interesting to note that the Hα emission is seen around a highly depleted hydrogen-deficient star. Hypothetically, this material could originate in *star_1* during a last phase of intense mass-transfer, and the hydrogen be stored during a long period of time in a stable accretion disk orbiting around the secondary.

4.3. Summary

The VEGA/CHARA observations provide stringent constraints that confirm the previous hypotheses proposed as an interpretation of time-variable spectroscopic observation of this source. Step by step we constructed a qualitative model that accounts for most of the VEGA/CHARA observation features. The findings are the following:

- 10–15% of the continuum flux originate from an extended source identified as a large circumbinary disk around the binary system.
- There is no clear sign of binarity in the absolute nor dispersed visibilities, constraining the flux contrast to a value higher than ∼4–5 between the relatively cool primary of the system and the hot component.

– Taking into account the extended flux contribution and assuming *star_2* to be unseen, the angular diameter of the primary is most probably in the range of 0.3–0.4 mas. At the Hipparcos distance this translates into a radius of 15−30 $R_\odot$, i.e. a radius much smaller than the estimated Roche radius of 80−130 $R_\odot$.
– The Hα emission is clearly off-center from the primary, and the Hα photocenter follows the position of the undetected secondary, located between the primary and the expected position for the secondary.
– The Hα line forming region is extended with a $FWHM$ larger than 3 mas, larger than the size of the system.

5. Non-conservative evolution of the υ Sgr and β Lyr systems

β Lyr and υ Sgr are two famous interacting binary systems. Currently, the orbital period of β Lyrae, P = 12.94 d is about 10 times shorter than the orbital period of υ Sgr, P = 137.9 d and slows down at a rate of 19 s per year. This slow-down is interpreted as an evidence of the non-conservative evolution of the system, i.e. that some mass is lost by the system during the mass transfer process. The study of the hydrogen and helium line forming regions of β Lyrae is also evidence of mass lost by the system. Assuming this rate is constant, the period may be doubled in about 60 000 yr, a relatively short time in view of stellar evolution scales and will reach υ Sgr's rate in about 6×10^5 yr, if this a high rate of mass-transfer is sustained. υ Sgr is more evolved than β Lyrae, exhibiting a hydrogen-deficient star that has been explained in the frame of a second mass-transfer stage. The mass-transfer of υ Sgr was also not conservative as shown by the large circumbinary disk that surrounds the system.

In the case of υ Sgr, the Hα line-forming region is much more extended than the scale of the system, and the photocenter of the Hα emission is located between the two stars, close to *star_2*. Given the intermediate inclination of the system, it is difficult to distinguish between the hydrogen emission lying in the equatorial plane and that outside. The large scale of the Hα formation region implies that a significant amount of mass is transfered from within the orbit to outside. Two main scenarios of mass-transfer need to be investigated in further studies: 1) a mass-transfer close to the orbital plane of the system, in which the dense and large circumbinary disk is fed continuously via the L2 Lagrangian point, forming perhaps a circumbinary disk of plasma; or 2) a mass-loss directed perpendicular to the orbital plane in the form of a jet, in which the radiative wind from the dense accretion disk around the gainer plays a significant role. These two processes are not exclusive and may have both played a significant role, however, the large separation of the components strongly limits the energetics of the mass transfer, and no sign of a "hot spot" has ever been reported for υ Sgr. Therefore, the mass-transfer via the equatorial plane is the favored mechanism.

A convincing example of this equatorial mass-transfer was reported for the binary system HD 62623 (Plets et al. 1995; Millour et al. 2011), an A-type supergiant with a solar-mass companion orbiting with a period P = 137.9 d. The SED and spectra from this system exhibit a large infrared excess and strong emission lines, respectively, and HD 62623 is classified as A[e]/B[e] source. Recent AMBER observations have shown that the Brγ line originates in a dense disk of plasma larger than the orbit of the secondary (Millour et al. 2011). The kinematics in the Brγ line is most probably Keplerian, suggesting that most of the mass-transfer occurs in this system close to the orbital plane. This is in line with the scenario proposed in Plets et al. (1995) in which the mass is transfered via the L2 Lagrangian point. The caveat of this scenario for υ Sgr is that the primary is hydrogen-deficient which seems a paradox to interpret the formation of this line as a transfer of hydrogen from the primary onto the accretion disk around the secondary. Moreover, the primary exhibits a diameter much smaller than the one inferred from the classical Roche-lobe approximation, and its temperature is not sufficient to sustain a strong and dense radiative wind. The accretion disk around the gainer is a reservoir of hydrogen and one may consider for υ Sgr that the Hα line is formed from strong radiative wind from the disk, and therefore mostly in the form of a jet-like feature. It must be noted that the photocenter of the Hα emission is located close to the secondary, which suggests that the accretion disk exerts a large influence on the launching mechanism.

Another interesting finding is that the *star_1* of υ Sgr is much smaller than the expected Roche-lobe radius. The forces acting within the system are numerous: the gravity from the stellar sources, the radiative flux from the stellar and non-stellar components (accretion disk...). In this context, it does not come as a surprise that the Roche-lobe approximation is not valid anymore, as discussed extensively in Dermine et al. (2009). The consequence of integrating many centripetal forces in the budget is a shrinking of the Roche-lobe, to the point that the Roche-lobe is not applicable anymore when these extra-forces dominate over the gravity from the stellar sources, i.e. in case of strong mass-loss from the system. This is probably the reason why the measured diameter of the primary of υ Sgr is so small.

The high inclination of the β Lyrae system makes it easier to show that the Hα, Hβ and HeI 6668 Å line forming regions are extended perpendicularly to the orbital plane, since the VEGA/CHARA baselines were oriented dominantly to the north-south direction. This was first seen by Harmanec et al. (1996) and Hoffman et al. (1998) and is confirmed here. The VEGA and NPOI observations suggest a limited opening angle of the jet-like feature, but this remains to be confirmed. The VEGA observations also provide further evidence that a large mass is currently lost by the system via the jets, and that a considerable part of the Hα, Hβ and HeI 6678 Å emission lines is formed within this structure. The mass transfered from the primary seems to violently encounter the dense, optically thick accretion disk that hides the secondary, creating the hot spot and escaping in the direction of least resistance, i.e. perpendicularly to the orbital plane. One may hypothesize that the mass lost by the system represents a substantial part of the mass-transfered currently from the primary in the direction of the secondary.

6. Conclusion

We presented VEGA/CHARA observations of two interacting massive binaries, β Lyrae and υ Sgr, containing a bright star and an unseen companion. These observations showed the huge extent of the Hα environment, larger than the scale of the orbits in both cases, giving evidence of a non-conservative evolution. The orbital period and separation of the systems considerably differ (by a factor ~10) and the VEGA observations confirm the large mass-loss rate via large opening angle jets for β Lyrae whereas an equatorial mass-loss is preferred for υ Sgr owing to the extended circumbinary disk that surrounds the stars.

These pilot observations, aiming at investigating the possibilities of the VEGA instrument, were performed by recombining two telescopes at a time. The high level of the continuum visibilities of both systems obtained with baselines reaching 100 m

implies that these sources are well suited to three or four telescope recombination, which necessarily implies the use of baselines in the range of 100–200 m, given the constraints from the configuration of the CHARA Array.

Acknowledgements. VEGA is a collaboration between CHARA and OCA/LAOG/CRAL/LESIA that has been supported by the French programs PNPS and ASHRA, by INSU and by the Région PACA. The CHARA Array is operated by Georgia State University with support from the National Science Foundation through grant AST-0908253, the W. M. Keck Foundation and from the NASA Exoplanet Science Institute. This research has made use of the Jean-Marie Mariotti Center `LITpro` and `SearchCal` services co-developed by CRAL, LAOG and FIZEAU, and of CDS Astronomical Databases SIMBAD and VIZIER. An anonymous referee is thanked, having provided pertinent advice that helped to improve this paper.

References

Ak, H., Chadima, P., Harmanec, P., et al. 2007, A&A, 463, 233
Bonneau, D., Clausse, J., Delfosse, X., et al. 2006, A&A, 456, 789
Chesneau, O., Dessart, L., Mourard, D., et al. 2010, A&A, 521, A5
De Greve, J. P., & Linnell, A. P. 1994, A&A, 291, 786
Delaa, O., Stee, P., Meilland, A., et al. 2011, A&A, 529, A87
Dermine, T., Jorissen, A., Siess, L., & Frankowski, A. 2009, A&A, 507, 891
Diaz-Cordoves, J., Claret, A., & Gimenez, A. 1995, A&AS, 110, 329
Dudley, R. E., & Jeffery, C. S. 1990, MNRAS, 247, 400
Eggleton, P. P. 2002, ApJ, 575, 1037
Harmanec, P. 2002, Astron. Nachr., 323, 87
Harmanec, P., Morand, F., Bonneau, D., et al. 1996, A&A, 312, 879
Hoffman, J. L., Nordsieck, K. H., & Fox, G. K. 1998, AJ, 115, 1576
Huang, W., & Gies, D. R. 2008, ApJ, 683, 1045
Koubský, P., Harmanec, P., Yang, S., et al. 2006, A&A, 459, 849
Leggett, S. K., Mountain, C. M., Selby, M. J., et al. 1986, A&A, 159, 217
Lomax, J. R., & Hoffman, J. L. 2011, Bull. Soc. Roy. Sci. Liège, 80, 689
Millour, F., Meilland, A., Chesneau, O., et al. 2011, A&A, 526, A107
Mourard, D., Clausse, J. M., Marcotto, A., et al. 2009, A&A, 508, 1073
Nariai, K. 1967, PASJ, 19, 564
Netolický, M., Bonneau, D., Chesneau, O., et al. 2009, A&A, 499, 827
Plets, H., Waelkens, C., & Trams, N. R. 1995, A&A, 293, 363
Rousselet-Perraut, K., Benisty, M., Mourard, D., et al. 2010, A&A, 516, L1
Schmitt, H. R., Pauls, T. A., Tycner, C., et al. 2009, ApJ, 691, 984
Schönberner, D., & Drilling, J. S. 1983, ApJ, 268, 225
Tallon-Bosc, I., Tallon, M., Thiébaut, E., et al. 2008, SPIE Conf. Ser., 7013
ten Brummelaar, T. A., McAlister, H. A., Ridgway, S. T., et al. 2005, ApJ, 628, 453
Umana, G., Maxted, P. F. L., Trigilio, C., et al. 2000, A&A, 358, 229
Umana, G., Leone, F., & Trigilio, C. 2002, A&A, 391, 609
van Leeuwen, F. 2007, A&A, 474, 653
Wolf, S., Henning, T., & Stecklum, B. 1999, A&A, 349, 839
Yudin, R. V. 2001, A&A, 368, 912
Zhao, M., Gies, D., Monnier, J. D., et al. 2008, ApJ, 684, L95